Biodegradable magnesium coronary stents: material, design and fabrication

Ali Gökhan Demir[a], Barbara Previtali[a]*,Qiang Ge[a], Maurizio Vedani[a], Wei Wu[b], Francesco Migliavacca[b], Lorenza Petrini[c], Carlo Alberto Biffi[d], Massimiliano Bestetti[b]

[a] *Dipartimento di Meccanica, Politecnico di Milano, Milan, Italy*

[b] *Dipartimento di Chimica, Materiali e Ingegneria Chimica "G. Natta", Politecnico di Milano, Milan, Italy*

[c] *Dipartimento di Ingegneria Civile e Ambientale, Politecnico di Milano, Milan, Italy*

[d]*CNR-IENI Unità di Lecco, Lecco, Italy*

*Corresponding author: Barbara Previtali. Dipartimento di Meccanica, Politecnico di Milano, Via La Masa 1, Milan, Italy. barbara.previtali@polimi.it

Biodegradable magnesium coronary stents: from the design to the realisation

Biodegradable cardiovascular stents in magnesium alloys constitute a promising option for a less intrusive treatment, due to their high compatibility to the body tissue and intrinsic dissolution in body fluids. The design and fabrication aspect of this medical device requires an integrated approach considering different aspects such as mechanical properties, corrosion behaviour and biocompatibility. This work gathers and summarizes a multi-disciplinary work carried out by three different research teams for the design and fabrication of magnesium stents. In particular the paper discusses the design of the novel stent mesh, the deformability study of the magnesium alloys for tubular raw material, and laser microcutting for the realization of the stent mesh. Although the results are not fully validated and the device fully tested, they show the feasibility of the used approaches, as the first prototype stents in magnesium alloy were produced successfully.

Keywords: cardiovascular stent; biodegradable, AZ31, tube extrusion, laser microcutting

Introduction

The efficacy of a medical device depends on several factors, which range from the proper identification of medical requirements, to the development of engineering solutions, and finally to the realization of the product itself. In the case of cardiovascular stents, the time scale between the conceptualization and the final implementation of the device is considerably longer, due to highly strict and demanding certification and clinical trial procedures. One of the main concerns regarding a cardiovascular stent application is the restenosis, which is the phenomenon of the arterial walls responding to the widening of the vessel to retrieve the previous patency due to a physiological response. The action called thrombosis manifests right after the

tissue damage caused by the insertion of the stent. Due to the damage, blood clot aggregates and causes immediate narrowing in the vessel. If the occlusion appears in 3-6 months after the implantation, the phenomenon is called in-stent restenosis and is due to inflammatory response of the body tissue to the stent presence. Preventing restenosis depends on the adequate design of the stent, but also on the chosen material which can ensure the biocompatibility with the body tissue. In particular the inclusion of elements in the stent material such as nickel, chrome, and molybdenum may trigger local immune response and inflammatory reactions, which may cause in turn the in-stent restenosis. Due to the importance of the material-body interactions, medical research has been widely focused on the material perspective to evaluate potential advantages and disadvantages of different alloys and elements as stent materials as well as the use of coatings to improve biocompatibility (Bertrand et al 1998, Lüscher et al 2007, Mani et al 2007, O'Brien and Carroll 2008). The restenosis risk along with long-term mechanical instabilities is evidently more crucial when the vessel grows in pediatric patients. The key to prevent such risk is bioabsorbability which is mainly dependant on the used stent material. The idea of using medical devices that fulfil their required duty and dissolve in human body in the due time, has resulted in extensive research attempts in material science, stent design and production fields. Biocompatibility, on the other hand, is the required property that ensures the body tissue to tolerate the material without causing inflammations, leading to a less intrusive treatment.

Magnesium, as an element already present in the human body, is highly compatible to the body tissues. Therefore, magnesium and its alloys as biodegradable and biocompatible implant materials represent a very attractive solution for their relatively low corrosion resistance in human body and for the good biocompatibility of both metal itself and the corrosion reaction products (Erne, Schier and Resink 2006,

Staiger et al 2006, Witte 2010). Moreover as a metal, magnesium provides better mechanical performance with respect to the polymeric biodegradable materials. Due to such advantages, the field has been receiving more attention from the scientific community, leading the research to some of the first clinical trials (Di Mario et al 2004, Zartner et al 2005, Waksman et al 2006). However, most of the literature currently deals with the advantages of the use of the biodegradable magnesium stents, whereas there is lack of information regarding the design and manufacturing aspects of a magnesium stent. The performance of the magnesium stent depends on an extensive study on all the main aspects, namely material, design and fabrication. Moreover, such a study requires a good synergy between all the steps, and iterations that starting from the correct material selection and stent design lead to the final product. These three phases indeed have to match together to obtain a good agreement between mechanical properties, corrosion resistance and biocompatibility. In the literature works that simultaneously treats these different aspects regarding the magnesium stent from the concept to the fabricated device are absent.

The present work investigates the overall realisation sequence of a new coronary stent in magnesium alloy based on a multidisciplinary approach that includes the three main aspects involved in the production of a new complex device: design, material and fabrication. The different aspects of the work were carried out by a research team that integrates together the three parts.

The whole chain of design and fabrication, from conceptualization to realization is demonstrated. The paper initially presents the multidisciplinary approach employed to link different aspects of the realization of the new biodegradable Mg stent, from conceptualization to realization. Then, the specific design and manufacturing methods employed to realize the biodegradable stents with a novel mesh design in AZ31

magnesium alloy are described. The new stent design was conceptualized and optimized through finite element analysis (FEA) for improved scaffolding properties. When the new stent was designed, the three main phases of the fabrication process were investigated: namely the extrusion of the precursor, the laser cutting of the stent mesh and finally the finishing operations. The extrusion capability of the AZ31 alloy was studied through hot compression tests. Determined parameters were used to extrude hollow small diameter tubes. The optimized mesh was cut on AZ31 tubes with 2.5 mm diameter and 0.2 mm thickness with a pulsed fiber laser. Chemical etching was applied on the material to remove the dross and re-molten material. The investigated sequence of steps enabling the production of magnesium alloy stents (MAS) puts in evidence the similarities of this procedure with the traditional one, and its own peculiarities, in the meantime offers extended insights to the industrialisation of this medical device.

1. The implemented multidisciplinary approach for the new stent design and fabrication

Three main aspects concerning a stent from conceptualization to realization can be identified as material, design, and fabrication (see Figure 1). For the specific case of biodegradable stents in Mg, the main issues concerning the three aspects can be listed as:

- Material - choice of Mg alloy type. Issues regarding toxicity, corrosion resistance, material resistance, recoil.
- Design of the mesh geometry. Issues regarding scaffolding ability, maximization of mass to control biodegradation rate.
- Fabrication - determining the production cycle. Feasible process with high dimensional precision, including the necessary finishing steps.

Although the roles of the three different aspects may seem discrete, they are in fact highly connected to the each other. The design of the stent is required to fully exploit the material characteristics, which should render the material a device that fulfils the certain duty of the stent. On the other hand, the design cannot reflect only the optimal geometric conditions to exploit the material mechanical properties to the highest, as long as it is not feasible for production. The fabrication methods should incorporate a production cycle capable of realizing and maintaining the material and design properties with required tolerance levels and quality, which reflect to the biocompatibility of the stent.

The multidisciplinary work on biodegradable magnesium stents compared these issues in three consecutive steps. Material selection was based on a compromise between the chemical, mechanical, and corrosion properties of the material, ease of manufacturing, and availability of the raw material. The design was based on 2D morphing algorithm to define the best dimensions to optimize scaffolding ability with increasing in stent mass. Fabrication steps were identified by adapting extrusion, laser microcutting and chemical etching processes to the peculiarities of the chosen magnesium alloy.

2. Choice of suitable Mg alloy

A variety of Mg alloys are available in extruded bar or sheet forms, which may include common alloying elements such as Al, Zn, or Mn; as well as rare earth (RE) metals such as Ce, Pr, or Nd. The alloying elements determine mechanical performance, as yield stress, ultimate tensile strength and elongation depend highly on the alloying compounds. Moreover, the alloying elements influence the corrosion behaviour of the material. As a matter of fact pure Mg has a very high corrosion rate in physiological pH (Steiger et al. 2006). Including rare earth metals can effectively improve the corrosion

resistance of the Mg alloy; however the low availability of the material is a concern that cannot be overseen. The formability of the alloy is another issue that needs to be addressed. Due to the low ductility of magnesium, the fabrication of tubular precursors in the dimensional range for a stent is difficult. Potentially, the chosen Mg alloy is supposed to exhibit a good compromise for the different aspects.

The magnesium alloys currently under investigation as biomedical materials are mostly commercial alloys which have been applied for industrial applications. Almost none of the mentioned alloys have been originally developed for biodegradable implant material. However, the specialization of magnesium alloys for biomaterial applications, including composition design, processing route and testing standards is already under development. According to designation system of American Society for Testing and Materials (ASTM) under the standard ASTM B296 - 03(2008), the magnesium-based alloys can be divided into three major groups: pure magnesium (Mg) with traces of other elements, Al-containing alloys and Al-free alloys (Polmear 1995). Due to the complex alloy composition and the limitations given by commercially available magnesium alloys, impurities (Ni, Cu, Fe and so on) may sum up to a total content of 0.3 wt.%. Very often these impurities are not listed in detail or even neglected. Although the given concentration of impurities are low compared to the physiological range in the body, the amount of these impurities has to be strictly controlled and kept at minimum level for biomedical applications. Elements such as beryllium and nickel should be avoided.

In order to obtain higher mechanical properties and corrosion resistance, the alloying elements listed in Table 1 are usually considered in magnesium alloys for biomedical applications. A brief summary for pathophysiological and toxicological characteristics of these alloying elements in human body were summarized by Witte et al. (Witte 2010). According to known effects, the summary given in Table 1 could be supplied. The

alloying elements to be added for developing biodegradable magnesium alloys are therefore limited to a few metals which are well known to be tolerated in the human body, including Ca, Zn, Mn and a small amount of RE. However, it is necessary to understand that the composition of alloy is even more complicated when rare earths are added to magnesium. Meanwhile, the processing routes should be strictly controlled in order to achieve the microstructural features required for high strength materials.

In this work AZ31 Mg alloy was chosen as the stent material. This alloy provides a good compromise between the mechanical properties and corrosion behaviour. Moreover, AZ31 shows good deformability providing conditions for extruding the material to small precursors, which can be later on laser micromachined to the required mesh design. The commercial availability of the alloy in form of extruded bars is another positive aspect. As a drawback the inclusion of aluminium in the alloy reduces the biocompatibility of the device.

3. A novel biodegradable Mg stent design

The new stent consisted of five rings connected by curved links, presenting six peak-to-valley struts in the circular direction (Figure 2.a). This design was the product of a shape optimization procedure that was carried out on the 2D geometry with a morphing procedure (Wu et al 2010). Briefly, an optimization algorithm was applied to an initial bi-dimensional geometry to control its shape with the use of FEA with the main aim of satisfying the two controversial demands, namely related to strain and mass, that a MAS has compared to conventional stainless steel (SS) stents. Indeed, SS stents undergo large local strain (about 0.4-0.5) during stent expansion, while most magnesium alloys have much lower ultimate elongation (usually below 0.2). Excessive strain of MAS during expansion needs to be avoided. Furthermore, the elastic modulus of magnesium alloys is about 25% of that of SS, thus a MAS needs more material (e.g.

widening stent strut) to provide adequate scaffolding. However, more material may also increase the strain during expansion. In an initial geometry, a strut unit was defined for optimization, with 3 main parts, curved (Cu), straight (St) and solidus (So) whose dimensions were varied to achieve geometry with the best performance (see Figure 2.c). The optimized design showed reduced maximum strain by 33% and increased scaffolding ability compared to an existing MAS design (Magic stent, Biotronic, Berlin, Germany) showed in Figure 2.b.

The new stent design was numerically compared to an existing stent (Wu et al 2011) in terms of degradation properties when virtually implanted in a vessel. For this purpose a continuum damage mechanics approach was applied (Gastaldi et al 2011). This approach takes into account both the uniform and the stress corrosion mechanisms. Indeed, these two aspects account for the micro galvanic mechanism experimentally observed in Mg alloys that results in corrosive attack uniformly distributed on the surface exposed to the aggressive environment and the localization of the corrosion attack in the areas of the material where the stress is more concentrated and the corrosion evolves mediated by the stress field. As seen in the FEM analysis reported in Figure 3, several parts of the conventional model are going to break (high damage locations indicated with red color), while the new stent model still keeps structural integrity. Results from this comparison showed that the new optimized stent design led to an increase of more than 100% in degradation time and accordingly it has improved scaffolding properties compared to the existing stent.

4. Fabrication of stents in AZ31 alloy

Cardiovascular stents are vastly produced by laser beam machining on tubular material, although they can be produced by many different processes which can involve braiding or knitting of wires, or cutting of tubular material by various methods such as electric

discharge machining (EDM) or water jet, or may involve deposition and casting techniques (Martinez and Chaikof 2007, Stoeckel et al 2002). A generic production cycle can include various steps, though laser microcutting is the main process that realizes the stent mesh on tubular material. Depending on the cut quality, the laser cut stent can require finishing processes such as initially chemical etching and then electrochemical polishing. Heat treatment and surface coating steps are optional depending on the stent material (Figure 4).

In the case of Mg stents, the production of the semi-finished tubular material plays a role as important as the consecutive machining of the stent mesh. In addition to the general difficulty of the extruding Mg alloys in the dimensions required for the stent applications, the extrusion process determines the microstructure of the material, which reflects to the corrosion behaviour of the stent in human body.

The following illustrates the first three steps, raw-material production, laser microcutting and chemical etching, as depicted in the generic stent production cycle scheme. Since, the last two involve the generation and the finishing of the stent geometry, they have been investigated together.

4.1. Extrusion of AZ31 tubes as stent precursors

The experimental materials used in this study was AZ31B magnesium alloy which was supplied in the form of commercially available wrought bars having a diameter of 15 mm. Hot-extrusion was carried out in the laboratory at die temperature of 410°C and average strain rate of $2.78 \cdot 10^{-3} s^{-1}$. A series of hollow tubes with outer diameter (D) ranging from 8 to 4 mm and inner diameter (d) from 6 to 3 mm were produced. The detailed experimental procedure for tube extrusion was reported in a previous work (Ge, Vedani, Vimercati 2012).

Texture evolution from the as received to the extruded materials was investigated by Electron Backscattering Diffraction (EBSD) technique. Specimens sectioned parallel to the extrusion direction were electro-polished to be ready for the analysis. To assess material performance strictly related to microstructural conditions matching the stent precursors, the mechanical properties were measured both in tension and compression on samples directly cut from extruded tubes to suitable gauge length. Tensile specimens had a gauge length of 30 mm for each extrusion diameter while compressive specimens had a reduced length of 20 mm to limit buckling phenomena during testing. For both of compressive and tensile modes, data were collected up to strain of 2% to avoid unwanted effects related to tube buckling in compression and sliding at grips in tension. After the tension-compression tests, microstructure was checked by optical and scanning electron microscopy to highlight possible modifications of microstructure induced by straining.

4.1.1. Microstructure

In Figure 5, the representative microstructure of extruded tube D4d3 is shown. Hereafter, the size of the tubes will be stated by a capital D followed by the size of the outer diameter and a d followed by inner diameter, both in mm. The micrographs are taken from mid-thickness of longitudinal sections of AZ31 samples. The concurrent action of temperature and strain during extrusion initially promoted recrystallization and a relatively more refined microstructure with equiaxed grains after extrusion (as depicted in Figure 5.a.). The orientation maps gathered from EBSD analysis revealed a preferred orientation in AZ31 extruded alloy as depicted in Figure 5.b. The map clearly reveals that the predominant red grains feature their (0001) planes aligned parallel to the sample surface (longitudinal axial sections).

Figure 6 shows the inverse pole figures in a direction normal to longitudinal axis obtained from starting alloy and after extrusion. It is revealed that AZ31 starting alloy had a condition with a weak texture given by the prismatic planes {10-10} and {2-1-10} aligned along the longitudinal axis of the bars (shown in Figure 6.a). After the laboratory-scale extrusion, the texture of the small-size tubes clearly changed as depicted in Figure 6.b. It is confirmed that a typical (0001) extrusion texture, featuring the basal plane aligned parallel to the extrusion direction was found in extruded tubes.

4.1.2. Mechanical Properties

Figure 7 depicts the initial part of the tensile and compression stress-strain curves recorded for AZ31 alloy. It is highlighted that yielding in compression occurs at significantly lower stress than in tension. Values of the 0.2% offset yield strength measured in tension and in compression are summarized in Table 2. Tests were performed on full-size cylindrical tube samples without machining a distinct gauge length due to small thickness limitations. Therefore, data about ultimate tensile strength and fracture elongation were not considered to be fully reliable and are not presented here.

It can be readily observed that both the materials before and after extrusion feature a marked tension-compression asymmetry, the tensile yield strength being always significantly higher than that in compression. Extrusion led to a more visible drop in compressive strength, which is still lower than that in as received alloy.

Studies about hcp crystal structure of magnesium (Wang and Huang 2007, Wu et al. 2010) reported that the basal slip systems available at room temperature for plastic deformation do not satisfy the Taylor criterion requiring five independent easy slip systems for homogeneous and generalized ductility of polycrystalline metals. Other non basal slip systems such as the prismatic and pyramidal slip would offer six extra

independent slip modes that could fulfil the requirement of plasticity and good workability. However, these non basal slip systems become available only at high temperature in Mg and Mg alloys (Lin, Hsu and Keh 2008) suggesting that shaping of the tubes cannot be performed other than by hot extrusion. The starting wrought bars here investigated exhibited weak preferential orientation of (10-10) and (2-1-10) planes along longitudinal direction. On the contrary, a well developed basal texture was found in the AZ31 alloy tubes from laboratory scale extrusion at 410°C.

In addition to dislocation slip, it was also reported that magnesium exhibits a strong propensity for mechanical twinning. Indeed, it is well known that twinning deformation modes play an important role during the deformation of hexagonal metals (Meyers, Vöhringer, and Lubarda 2001). Despite the limited contribution of twinning itself to the total plasticity, the abrupt change of orientation due to twinning may give rise to the activation of other slip systems. The {10-12} <10-11> twin system is often observed in magnesium alloys and considered to be the preferential twinning system (Choudhary et al 2011). This kind of twinning preferably occurs when shear results from compressive stress applied parallel to the basal plane or from tensile stress applied perpendicularly to the same plane Wang and Huang 2007). By the texture condition detected in the present extruded tubes, crystallographic orientation in the sample does not allow easy twinning under tensile loading but twinning becomes favoured under compressive loading. Accordingly, the {10-12}<10-11> twinning was activated under compressive stress but not in tensile stress along the extrusion directions of the tubes, which resulted in abrupt decrease of yield stress in compression and marked compressive-tensile asymmetric behaviour. The occurrence of twinning was also clearly detected by metallographic observations (Vedani, Ge, Wu, and Petrini, 2012).

4.2. Laser microcutting of the stent mesh on AZ31 and chemical etching

Laser microcutting of cardiovascular stents is traditionally done using pulsed lasers that enable cut kerfs of a few tens of micrometers which is essential in order to realize such fine geometries (Dubey and Yavada 2008, Kathuria 2005, Raval et al 2004). On the other hand, pulse duration along with the laser wavelength is the most important aspects that determine the cut quality. Lasers operating in *m*s-*µs* are the industrially applied solutions for stent cutting due to their high productivity. However *m*s-*µs pulse* durations produce lower cut quality as well as a high amount of dross and heat affection of processed material due to longer pulse durations. Lasers with *ps-fs* ultra-short pulses on the other hand supply a very high cutting quality due to ablation based process (Momma, Knop and Nolte 1999, Muhammad et al 2011), but they are not industrially diffused and are costly solutions. Meanwhile, *ns* pulse regime is a domain that has received little attention so far, even though its potentiality for a good trade off between high productivity and high quality.

In this study focussed on cutting of the stent mesh, an active fiber laser operating in ns pulse regime with 50 W maximum average power (IPG- YLP-1/100/50/50) was used. In Table 3 the main specifications of the laser source are reported. The laser source was coupled with a cutting head (LaserMech) that housed a 60 mm focusing lens and a nozzle for process gas addition. In this configuration the obtained beam spot was 23 µm, which allowed microcutting with small kerf widths. For positioning a linear and a rotary axis (Aerotech ALS and ACS series) with nanometric resolution were used. The microcutting setup is reported in detail in Figure 8.

For the experiments, AZ31 tubes in 2.5 mm outer diameter and 0.2 mm thickness were used. Compared to the more traditional stent material stainless steel, which is commonly cut with oxygen, magnesium alloys require different laser microcutting conditions. Due to high melting temperature of the MgO, laser microcutting with

oxygen as process gas was not found to be a feasible option. Such conditions result in uncut sections due to the generated oxide layer in the kerf (Demir et al. 2012). Therefore, cutting with an inert gas is an essential requirement working with magnesium alloys.

An average power of 7.5 W with 25 kHz pulse repetition rate was found suitable for the cutting operation. Argon was used as assist gas with 7 bar pressure (purity 99.998%), and cutting speed of 2 mm/s was employed. An acidic solution of HNO_3 (65% purity) 10 mL, ethanol 90 mL was preferred for chemical etching in order to remove dross and to clean the kerf, which was previously demonstrated to effectively remove dross on laser microcut AZ31 sheets (Lesma et al 2010). The complete separation as well as mesh strut polishing was aimed to be achieved by applying the etching solution. Figure 9.a reports a SEM image of the AZ31 stent after laser microcutting. It can be observed that along the kerf area dross is present to a limited extent. A small amount of spatter is also evident near to cutting zones. The AZ31 stent after chemical etching is reported in Figure 9.b. It can be seen that the chemical etching successfully removed the dross on the surface, as the stent surface is clearly free of defects. However, along the stent thickness the walls show a roughness compared to the stent surfaces, which implies that the stent requires a further chemical polishing step to remove the asperities. On the other hand, the mesh design has been reproduced on the tube with high precision.

5. Conclusion

The present study describes the design and realization steps of a biodegradable and biocompatible stent in AZ31 alloy. Three main aspects to realize the biodegradable stent from the conceptual stage to the product have been identified as material, design and fabrication. A multi-disciplinary approach that incorporates different roles of material, design and fabrication research teams for the requirements of mechanical

properties, production cycle and manufacturability issues has been employed. Following to this, the steps that involve the alloy selection, the design optimization, and the study of the AZ31 magnesium alloy for semi-finished tube extrusion and the realization of the final stent through laser microcutting and chemical etching have been explained. Specifically, the following conclusions can be drawn:

- Among different magnesium alloys, AZ31 constitutes a good compromise between different material requirements, manufacturability and availability.
- Stent design plays a critical role for mechanical properties and corrosion performance; shape optimization can potentially increase the maximum strain and scaffolding ability.
- Preliminarily hot compression tests and laboratory extrusions allowed producing precursors of stents in the form of small tubes featuring a fine and equiaxed grain structure with increased hardness over the starting alloy.
- Laser microcutting with a pulsed fiber laser is a suitable solution to cut AZ31. The relatively longer ns pulses result in a limited amount of dross around and inside the kerf.
- Chemical etching with a HNO_3 – ethanol solution is able to clean the dross and complete the scrap separation. The obtained stent requires further electropolishing stage to increase the edge quality.

As a result of this multi-disciplinary work, the first prototype stents have been produced; this confirmed the feasibility of the applied approach. The control of the biodegradation rate is one of the points requiring further attention. The attempts of our research group will be focused to decelerate the corrosion rate of Mg alloy stents. For this purpose, the solutions involving the optimization of the microstructure of the raw material, the surface structuring and the adhesion of a biopolymer coating will be

studied. In-vitro degradation of the stent materials will be evaluated for the choice of optimal combination of these solutions to be applied on the stent geometry. The interaction between the stent geometry and plausible combinations of the methods for optimizing the corrosion behaviour will be investigated by means of FEM simulations before animal trials and in vivo tests will be carried out.

Acknowledgements

The authors would like to express their gratitude to Fondazione CaRiTRO for partially funding the research under grant number 2011.0250.

References

Bertrand, O. F. et al, 1998. "Biocompatibility Aspects of New Stent Technology." *Journal of the American College of Cardiology* 32 (3) : 562–71.

Choudhary, L., Szmerling, J., Goldwasser, R., Raman, R.K.S., 2011. Investigations into stress corrosion cracking behaviour of AZ91D magnesium alloy in physiological environment. Proc. Eng. 10, 518-523.

Demir, A.G. et al., 2012. Fiber laser micromachining of magnesium alloy tubes for biocompatible and biodegradable cardiovascular stents, In *Proceedings of SPIE*, 8237, pp.823730–823730–9.

Di Mario, C. et al. 2004. "Drug-eluting Bioabsorbable Magnesium Stent." *Journal of Interventional Cardiology* 17 (6) (December): 391–5.

Dubey, A.K., and Yadava V. 2008. "Laser Beam machining—A Review." *International Journal of Machine Tools and Manufacture* 48 (6).

Erne, P., Schier M., and Resink T.J.. 2006. "The Road to Bioabsorbable Stents: Reaching Clinical Reality?" *Cardiovascular and Interventional Radiology* 29 (1): 11–6.

Farè, S. et al., 2010. Evaluation of material properties and design requirements for biodegradable magnesium stents. *Matéria*, 15(2), pp.96–103

Gastaldi et al. 2011. "Continuum damage model for bioresorbable magnesium alloy devices — Application to coronary stents". Journal of the Mechanical Behavior of Biomedical Materials, S4 352 – 365

Ge Q., Vedani M. and Vimercati G. 2012. “Extrusion of Magnesium Tubes for Biodegradable Stent Precursors”. *Materials and Manufacturing Processes* 27 (2) 140-146

Kathuria, Y.P. 2005. “Laser Microprocessing of Metallic Stent for Medical Therapy.” *Journal of Materials Processing Technology* 170 (3) 545–550.

Lesma, E. et al., 2010. “Manufacturing of biocompatible magnesium stent mesh using nanosecond fiber laser and chemical etching”. In *Proceedings of 2nd Symposium on Biodegradable Metals*. pp. 82–83.

Lin, H., Hsu, Y., Keh, C., 2008. Inhomogeneous deformation and residual stress in skin-pass axisymmetric drawing. Jour. Mater. Proc. Tec. 201, 128-132.

Lüscher, T. et al. 2007. “Drug-eluting Stent and Coronary Thrombosis: Biological Mechanisms and Clinical Implications.” *Circulation* 115 (8): 1051–8.

Mani, G., Feldman M.D., Patel D., and Agrawal C.M. 2007. “Coronary Stents: a Materials Perspective.” *Biomaterials* 28 (9) (March): 1689–710.

Martinez, A.W., and Chaikof E.L. 2011. “Microfabrication and Nanotechnology in Stent Design.” *Wiley Interdisciplinary Reviews. Nanomedicine and Nanobiotechnology* 3 (3): 256–68.

Meyers M.A., Vöhringer O., and Lubarda V.A. 2001 “The onset of twinning in metals: a constitutive description.” *Acta Mater* 49:4025–4039

Momma, C, Knop U., and Nolte S. 1999. “Laser Cutting of Slotted Tube Coronary Stents – State-of-the-Art and Future Developments.” *Progress in Biomedical Research* 4 (1): 39–44.

Muhammad, N., et al. 2011. “Picosecond Laser Micromachining of Nitinol and Platinum–iridium Alloy for Coronary Stent Applications.” *Applied Physics A* 106 (3): 607–617.

O’Brien, B., and Carroll W. 2009. “The Evolution of Cardiovascular Stent Materials and Surfaces in Response to Clinical Drivers: a Review.” *Acta Biomaterialia* 5 (4): 945–58.

Polmear, I.J.,1995, *Light alloys, Metallurgy of the light metals*. Arnold

Raval, A., Choubey, A., Engineer C., and Kothwala D. 2004. “Development and Assessment of 316LVM Cardiovascular Stents.” *Materials Science and Engineering: A* 386 (1-2): 331–343.

Staiger, Pietak, Huadmai, Dias, 2006. Magnesium and its alloys as orthopedic biomaterials: A review, Biomaterials 27: 1728-1734

Stoeckel, D, Bonsignore C., Duda S. 2002. "A Survey of Stent Designs." *Minimally Invasive Therapy & Allied Technologies : MITAT : Official Journal of the Society for Minimally Invasive Therapy* 11 (4): 137–47.

Vedani M., Ge Q., Wu W. and Petrini L. 2012. "Texture effects on design of Mg biodegradable stents." *International Journal of Material Forming*, DOI 10.1007/s12289-012-1108-5

Waksman, R. et al. 2006. "Safety and Efficacy of Bioabsorbable Magnesium Alloy Stents in Porcine Coronary Arteries." *Catheterization and Cardiovascular Interventions : Official Journal of the Society for Cardiac Angiography & Interventions* 68 (4): 607–17

Witte F., Hort N., Vogt C., Cohen S., Kainer K.U., Willumeit R., Feyerabend F. 2008. "Degradable biomaterials base on magnesium corrosion." *Current Opinion in Solid State and Materials Science* 12, 63-72.

Witte, F. 2010. "The History of Biodegradable Magnesium Implants: a Review." *Acta Biomaterialia* 6 (5), 1680–92.

Wu, W, et al. 2010. "Finite Element Shape Optimization for Biodegradable Magnesium Alloy Stents." *Annals of Biomedical Engineering* 38 (9).

Wu, W. et al., 2011. Finite element analyses for design evaluation of biodegradable magnesium alloy stents in arterial vessels. *Materials Science and Engineering: B*, 176(20), pp.1733–1740.

Zartner, P., Cesnjevar R., Singer H., Weyand M. 2005. "First Successful Implantation of a Biodegradable Metal Stent into the Left Pulmonary Artery of a Preterm Baby." *Catheterization and Cardiovascular Interventions : Official Journal of the Society for Cardiac Angiography & Interventions* 66 (4)

Tables

Table 1. Summary of the toxicology and pathophysiology of alloying elements. Adapt from Witte et al. 2008

Element	Pathophysiology/toxicology Alloying Elements
Magnesium	Normal blood serum level 0.73–1.06 mmol/L; Influences growth factor effectiveness; Co-regulator of energy metabolism, cell proliferation, protein synthesis, onset of DNA synthesis; Regulator of more than 350 proteins; Stabilizer of DNA and RNA ; Long-term influence on cellular reactions ; Cellular up-take via transient receptor potential (TRP) ion channels ; Co-regulator and activator of integrins (cell migration) .
Calcium	Normal serum level 0.919–0.993 mg/L; Most abundant mineral in the human body (1–1.1 kg) ; Mainly stored in bone, teeth ; Is tightly regulated by homeostasis of skeletal, renal and intestinal mechanism.
Aluminum	Normal blood serum level 2.1–4.8 lg/L; Established alloying element in titanium implants; Risk factor in generation of Alzheimer's disease; Can cause muscle fiber damage; Decrease osteoclast viability; In magnesium alloys: mild foreign body reactions were observed in vivo.
Zinc	Normal blood serum level 12.4–17.4 lmol/L; Trace element; Essential for the immune system; Co-factor for specific enzymes in bone and cartilage; Neurotoxic at higher concentrations.
Manganese	Normal blood serum level <0.8 lg/L;

	Essential trace element; Important role in metabolic cycle of e.g. lipids, amino acids and carbohydrates; Influences the function of the immune system, bone growth, blood clotting, cellular energy regulation and neurotransmitter synthesis; Scavenger of free radicals in the manganese superoxide dismutase; Neurotoxic in higher concentration (manganism).
Lithium	Normal blood serum level 2–4 ng/g; Compound of drugs for treatment of psychiatric disorders; Overdosage causes nephrological or lung dysfunctions; Possible teratogenic effects.
Rare earth elements	Many rare earth elements exhibit anticancerogenic properties.

Table 2. Tensile and compression 0.2% offset yield strength of the as received bars and extruded tubes.

	As Received	Tube D6d3
Compressive Yield Stress (MPa)	109.6	91.8
Tensile Yield Stress (MPa)	149.7	166.5
Loss of yield strength (compression vs. tension, in %)	26.8	44.9

Table 3. Specifications of the laser microcutting system.

IPG YLP-1/100/50/50 Q- switched laser	
Laser wavelength	1064 nm
Maximum average power	50 W
Maximum pulse energy	1 mJ
Minimum pulse duration [FWHM]	100 ns
Pulse repetition rate	20-80 kHz
Beam quality factor (M^2)	1.7
Focused laser beam diameter	23 µm

High precision positioning system	
Spindle accuracy	±72.7 µrad
Linear axis accuracy	1 µm

List of figures

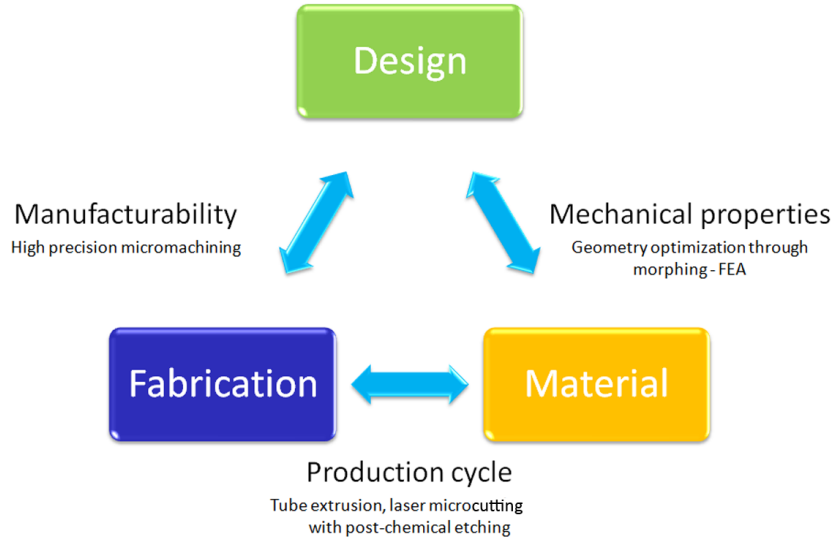

Figure 1. The aspects and interactions within the multi-disciplinary approach used in the design and fabrication of the biodegradable Mg stents

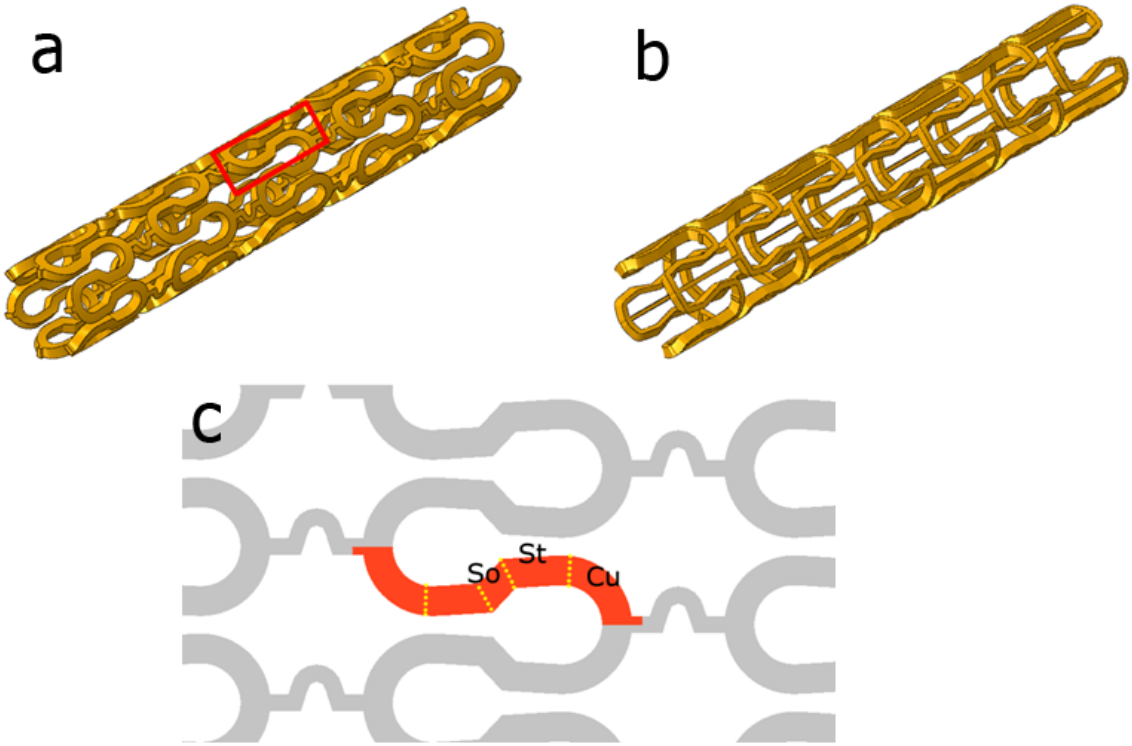

Figure 2. CAD models showing a) an existing coronary magnesium stent; b) of the new stent in the original configuration; and c) 2D dimensions of the new stent after shape optimization (adapted with permission from Wu et al).

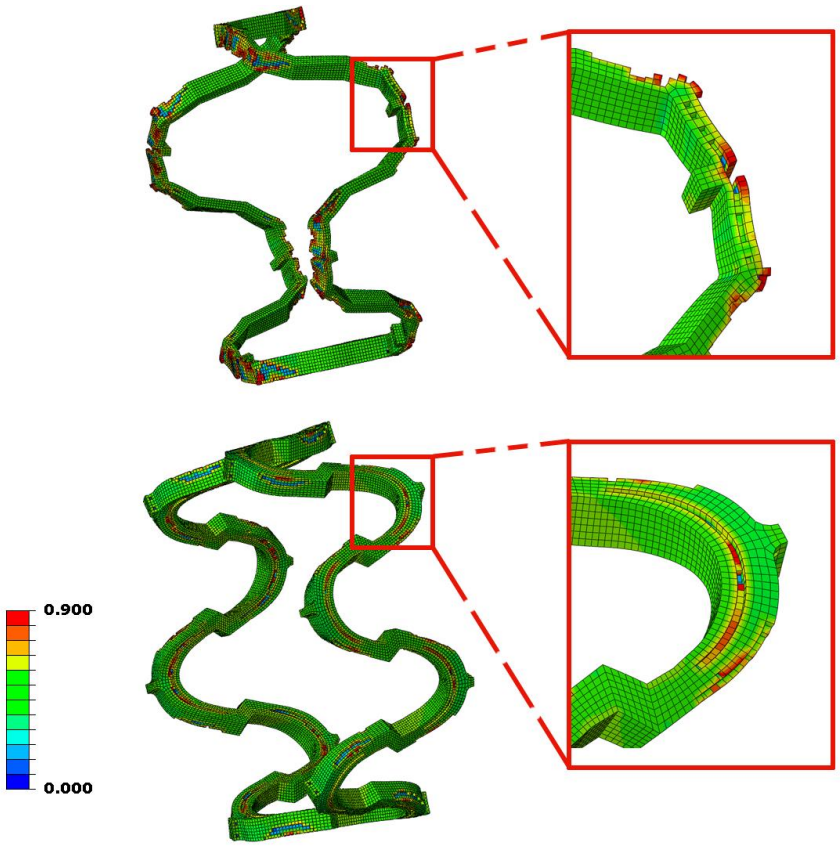

Figure 3. The comparison of degradation process of a conventional stent (upper panel) and the new stent design (lower panel) at the same degradation time using FEA. The legend indicates damage parameter with 0 meaning intact and 0.9 totally damaged.

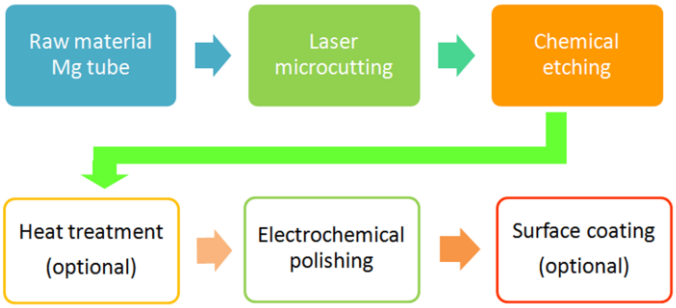

Figure 4. Production cycle of a cardiovascular stent. The process steps involved in this study are reported in the upper row.

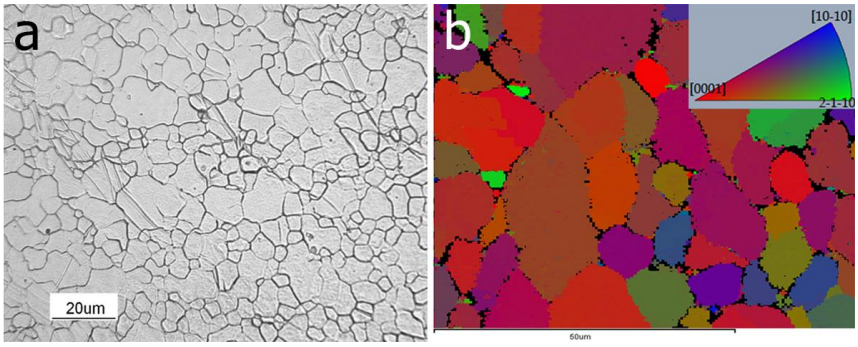

Figure 5. Microstructure of extruded D4d3 AZ31 tube on longitudinal section: a) optical micrograph; b) Orientation map from EBSD.

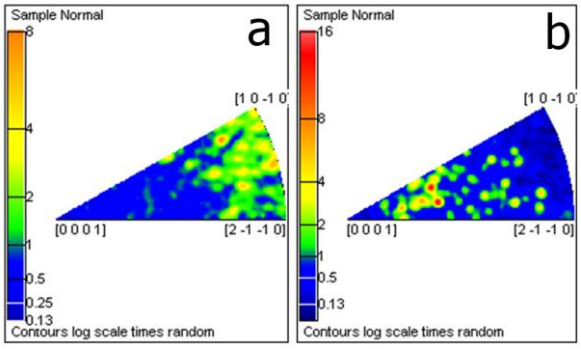

Figure 6. Inverse pole figures taken from longitudinal sections of : a) The starting bar; b) Extruded tube.

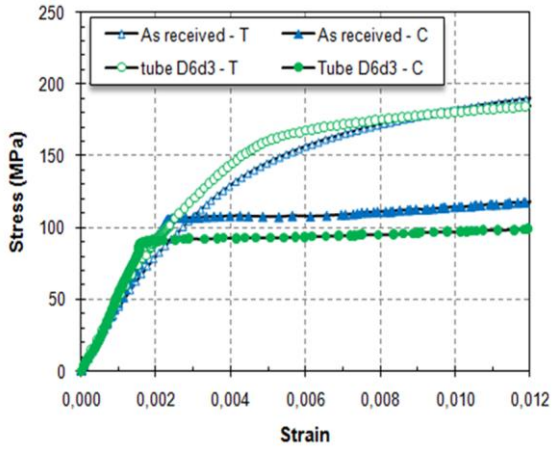

Figure 7. Tensile (T) and compression (C) stress-strain curves detected on starting bars and on hot-extruded tubes.

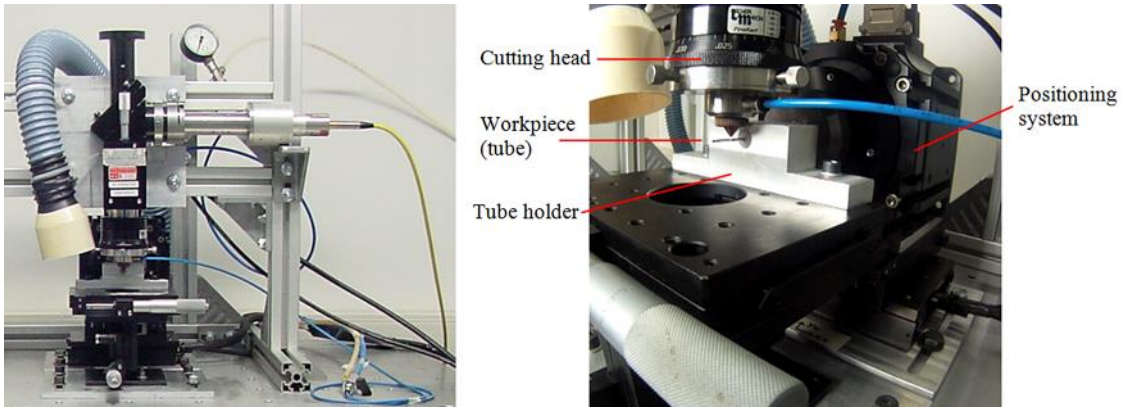

Figure 8. Laser microcutting system.

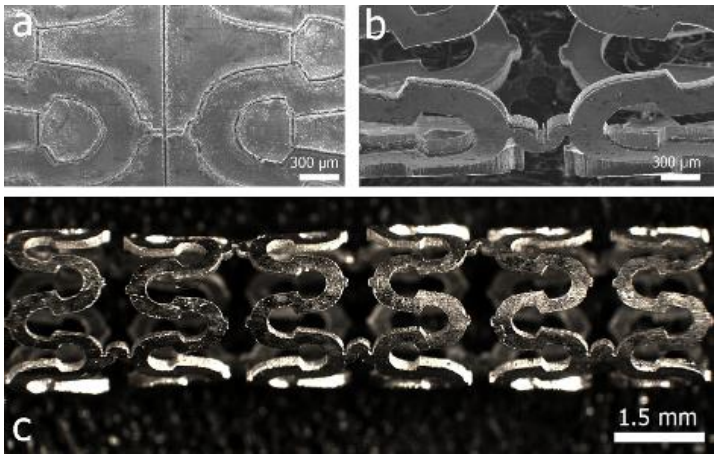

Figure 9. SEM images of the biodegradable AZ31 stent a) after laser microcutting, b) after chemical etching. c) Optical microscopy image of the stent